IUCrJ

Volume 8 (2021)

**Supporting information for article:**

# Relativistic Hirshfeld atom refinement of an organo-gold(I) compound

**Sylwia Pawlędzio, Maura Malinska, Magdalena Woińska, Jakub Wojciechowski, Lorraine Andrade Malaspina, Florian Kleemiss, Simon Grabowsky and Krzysztof Woźniak**

**S1. Meindl-Henn fractal dimensions plots**

For good quality data, a Gaussian distribution (Schwarzenbach *et al.*, 1989) of the residual electron density in the unit cell is expected. The most common method used in crystallography, which describes distribution of the residual density is the so-called Meindl-Henn fractal dimension plot. In this technique, the dimension of the residual density isosurface of constant value is defined by a method called the box-counting dimension or Hausdorff dimension $d^f$, and is defined according to Bronstein *et al.* (Bronstein *et al.*, 2008):

$$d^f(\rho_0) = x = \lim_{\varepsilon \to 0} \frac{\log N(x,\ \varepsilon)}{\log N\ (\frac{1}{\varepsilon})}$$

where ε is the length of a box covering the unit cell under consideration, and N(x, ε) is the number of boxes which contain unit cell. For a theoretical data, where no noise is present and model describes electron density ideally ($F_{obs} = F_{calc}$), the isosurface of $\rho_0 = 0$ eÅ$^{-3}$ fill unit cell completely with a $d^f$ equal to 3. If only noise is present in the data, but no model errors are present, positive and negative residual density appears. In this case, the shape of the fractal dimension plot is parabolic. The upper limit of the $d^f$ at $\rho_0 = 0$ eÅ$^{-3}$ decreases to a non-integer value, which is characteristic for any experimental case. The value of $d^f$ at $\rho_0 = 0$ eÅ$^{-3}$ indicates featurelessness (the higher value, the less features) in the distribution of residual density. The difference between the values of maximum and minimum residual density corresponds to the flatness of the distribution of residual density (the lower difference, the flatter distribution).

**References:**

Schwarzenbach, D., Abrahams, S. C., Flack, H. D., Gonschorek, W., Hahn, T., Huml, K., Marsh, R. E., Prince, E., Robertson, B. E., Rollett, J. S. & Wilson, A. J. C. (1989). *Acta Cryst A*. **45**, 63–75.

Bronstein, I. N., Semendjajew, K. A., Musiol, G. & Muehlig, H. (2008). Taschenbuch der Mathematik Frankfurt am Main: Deutsch.

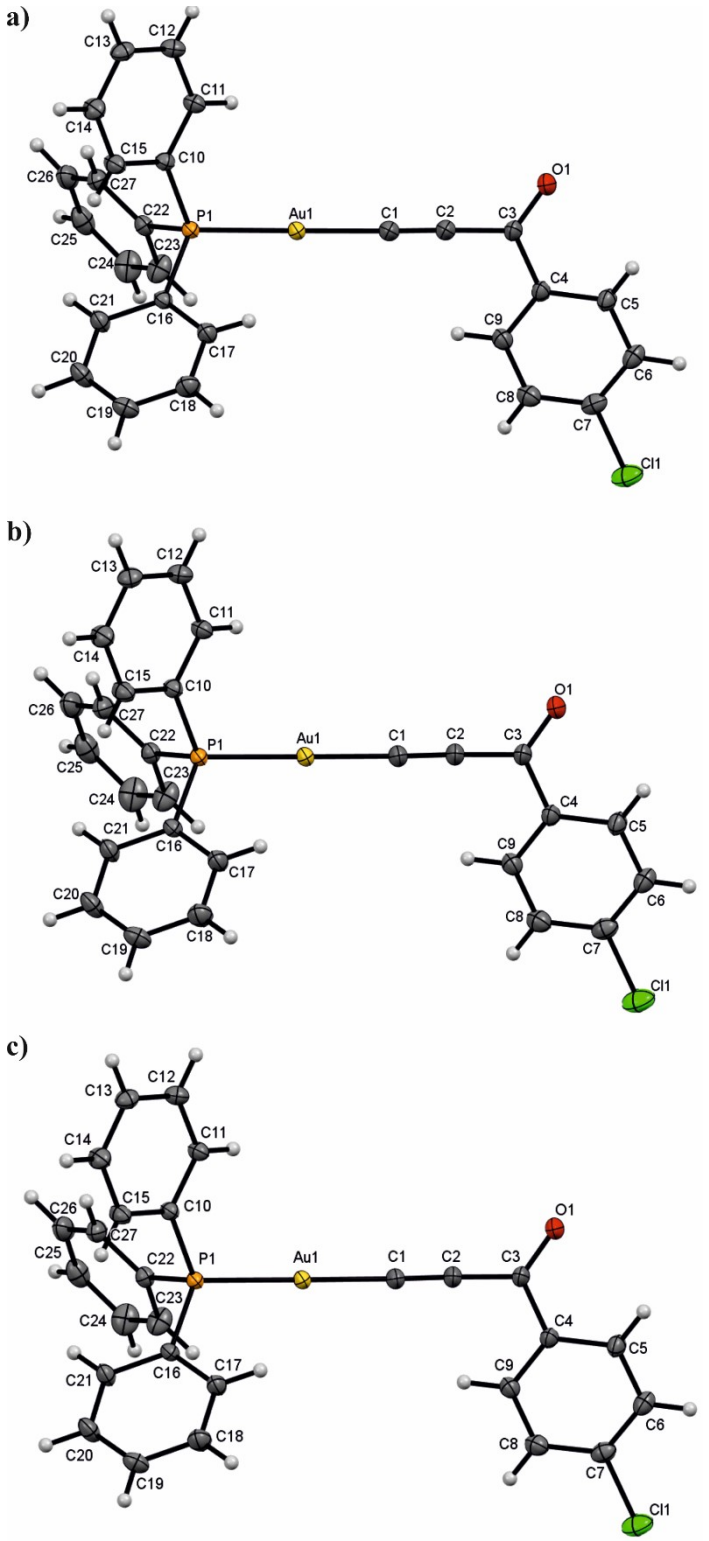


**Figure S1** ORTEP-style representation of the molecule for the (a) Ag, (b) Mo and (c) SP8 data after IAM with labelling scheme. Ellipsoids are drawn at 50% probability level. H atoms are shown as small spheres of arbitrary radius.

**Table S1** Statistical parameters of the HARs for the Ag data.

| | rks-anh_nr | rks_rel | rhf-anh_rel | rks-anh_rel |
|---|---|---|---|---|
| **R_sig(F)** | 2.72% | 2.72% | 2.72% | 2.72% |
| **R_sig($F^2$)** | 0.11% | 0.11% | 0.11% | 0.11% |
| **R(F)** | 1.59% | 1.71% | 1.57% | 1.59% |
| **R($F^2$)** | 1.49% | 1.73% | 1.46% | 1.50% |
| ***w*R (F)** | 1.78% | 1.90% | 1.76% | 1.78% |
| ***w*R ($F^2$)** | NaN | NaN | NaN | NaN |
| **N_r** | 11101 | 11101 | 11102 | 11101 |
| **N_p** | 381 | 356 | 381 | 381 |
| **$\chi^2$** | 0.965 | 1.101 | 0.951 | 0.970 |
| **GooF** | 0.983 | 1.049 | 0.975 | 0.980 |
| **Effective (mean) $\sigma^2$** | 0.0835 | 0.0790 | 0.0840 | 0.0836 |
| **Scale** | 0.1226 | 0.1214 | 0.1229 | 0.1225 |
| **$\rho_{max}$** | 0.63 | 1.66 | 0.63 | 0.63 |
| **$\rho_{min}$** | -0.58 | -0.62 | -0.54 | -0.58 |

**Table S2** Statistical parameters of the HARs for the Mo data.

| | **rks-anh_nr** | **rks_rel** | **rhf-anh_rel** | **rks-anh_rel** |
|---|---|---|---|---|
| **R_sig(F)** | 3.17% | 3.17% | 3.17% | 3.17% |
| **R_sig($F^2$)** | 0.14% | 0.14% | 0.14% | 0.14% |
| **R(F)** | 1.91% | 2.31% | 1.91% | 1.92% |
| **R($F^2$)** | 1.55% | 2.62% | 1.56% | 1.59% |
| ***w*R (F)** | 2.01% | 2.33% | 2.01% | 2.01% |
| ***w*R ($F^2$)** | NaN | NaN | NaN | NaN |
| **N_r** | 19255 | 19255 | 19255 | 19255 |
| **N_p** | 381 | 356 | 381 | 381 |
| **$\chi^2$** | 1.506 | 2.019 | 1.494 | 1.500 |
| **GooF** | 1.227 | 1.421 | 1.222 | 1.220 |
| **Effective (mean) $\sigma^2$** | 0.0336 | 0.0364 | 0.0339 | 0.0341 |
| **Scale** | 0.1231 | 0.1197 | 0.1231 | 0.1227 |
| **$\rho_{max}$** | 0.98 | 3.54 | 1.01 | 1.06 |
| **$\rho_{min}$** | -0.89 | -0.97 | -1.18 | -0.97 |

**Table S3** Statistical parameters of the HARs for the SP8 data.

| | rks-anh_nr | rks_rel | rhf-anh_rel | rks-anh_rel |
|---|---|---|---|---|
| **R_sig(F)** | 2.52% | 2.52% | 2.52% | 2.52% |
| **R_sig($F^2$)** | 0.04% | 0.04% | 0.04% | 0.04% |
| **R(F)** | 1.80% | 1.96% | 1.79% | 1.80% |
| **R($F^2$)** | 2.33% | 2.73% | 2.33% | 2.38% |
| ***w*R (F)** | 2.78% | 2.91% | 2.78% | 2.78% |
| ***w*R ($F^2$)** | NaN | 216.72% | NaN | NaN |
| **N_r** | 23104 | 23102 | 23103 | 23102 |
| **N_p** | 381 | 356 | 381 | 381 |
| **$\chi^2$** | 1.766 | 1.927 | 1.761 | 1.760 |
| **GooF** | 1.329 | 1.388 | 1.327 | 1.330 |
| **Effective (mean) $\sigma^2$** | 0.0694 | 0.0675 | 0.0694 | 0.0699 |
| **Scale** | 0.1224 | 0.1210 | 0.1223 | 0.1220 |
| **$\rho_{max}$** | 1.13 | 3.30 | 1.14 | 1.20 |
| **$\rho_{min}$** | -0.88 | -1.01 | -0.82 | -0.84 |

**Table S4** Bond lengths of the Au-P and Au-C after HARs.

| | Ag | | Mo | | Synchrotron | |
|---|---|---|---|---|---|---|
| | **Au1-P1** | **Au1-C1** | **Au1-P1** | **Au1-C1** | **Au1-P1** | **Au1-C1** |
| **rks-anh_nr** | 2.2742(2) | 1.9896(10) | 2.27255(18) | 1.9854(7) | 2.27732(19) | 1.9892(7) |
| **rhf-anh_rel** | 2.2741(2) | 1.9886(10) | 2.27255(18) | 1.9856(7) | 2.27718(19) | 1.9887(7) |
| **rks_rel** | 2.2733(3) | 1.9892(10) | 2.2725(2) | 1.9851(8) | 2.27674(19) | 1.9890(8) |
| **rks-anh_rel** | 2.2742(2) | 1.9884(10) | 2.27255(18) | 1.9854(7) | 2.27726(19) | 1.9887(7) |

**Table S5** C–H bond lengths after HARs for the Ag data.

| | **rks-anh_nr** | **rhf-anh_rel** | **rks_rel** | **rks-anh_rel** |
|---|---|---|---|---|
| C5–H5 | 1.14(2) | 1.14(2) | 1.13(2) | 1.14(2) |
| C6–H6 | 1.09(2) | 1.09(1) | 1.14(1) | 1.09(1) |
| C8–H8 | 1.06(2) | 1.06(2) | 1.06(2) | 1.06(2) |
| C9–H9 | 0.99(2) | 0.97(2) | 1.07(2) | 0.98(2) |
| C11–H11 | 1.08(2) | 1.08(2) | 1.10(2) | 1.08(2) |
| C12–H12 | 1.09(2) | 1.09(2) | 1.05(2) | 1.09(2) |
| C13–H13 | 1.03(2) | 1.01(2) | 0.98(2) | 1.03(2) |
| C14–H14 | 1.00(2) | 1.00(2) | 1.02(2) | 1.00(2) |
| C15–H15 | 1.08(2) | 1.08(2) | 1.09(2) | 1.08(2) |
| C17–H17 | 1.04(2) | 1.04(2) | 1.04(2) | 1.04(2) |
| C18–H18 | 1.15(2) | 1.14(2) | 1.13(2) | 1.14(2) |
| C19–H19 | 1.11(2) | 1.12(2) | 1.07(2) | 1.11(2) |
| C20–H20 | 1.12(2) | 1.13(2) | 1.10(2) | 1.12(2) |
| C21–H21 | 1.11(2) | 1.11(2) | 1.15(2) | 1.11(2) |
| C23–H23 | 1.11(2) | 1.11(2) | 1.19(2) | 1.11(2) |
| C24–H24 | 1.21(2) | 1.20(2) | 1.19(2) | 1.21(2) |
| C25–H25 | 1.15(2) | 1.14(2) | 1.18(2) | 1.15(2) |
| C26–H26 | 1.12(2) | 1.12(2) | 1.16(2) | 1.12(2) |
| C27–H27 | 1.14(2) | 1.12(2) | 1.15(2) | 1.14(2) |
| $\mathbf{C_{avr}}$ | 1.09(2) | 1.09(2) | 1.11(2) | 1.09(2) |

**Table S6** C–H bond lengths after HARs for the Mo data.

| | **rks-anh_nr** | **rhf-anh_rel** | **rks_rel** | **rks-anh_rel** |
|---|---|---|---|---|
| C5–H5 | 1.12(2) | 1.12(2) | 1.13(2) | 1.12(2) |
| C6–H6 | 1.12(2) | 1.13(2) | 1.12(2) | 1.12(2) |
| C8–H8 | 1.07(2) | 1.08(2) | 1.08(2) | 1.07(2) |
| C9–H9 | 1.08(2) | 1.08(2) | 1.07(2) | 1.08(2) |
| C11–H11 | 1.14(2) | 1.14(2) | 1.14(2) | 1.14(2) |
| C12–H12 | 1.05(2) | 1.04(2) | 1.03(2) | 1.05(2) |
| C13–H13 | 1.11(2) | 1.12(2) | 1.11(3) | 1.11(2) |
| C14–H14 | 1.03(2) | 1.03(2) | 1.04(3) | 1.03(2) |
| C15–H15 | 1.07(2) | 1.07(2) | 1.06(2) | 1.07(2) |
| C17–H17 | 1.04(2) | 1.05(2) | 1.03(2) | 1.04(2) |
| C18–H18 | 1.09(3) | 1.08(3) | 1.08(2) | 1.09(3) |
| C19–H19 | 1.11(2) | 1.11(2) | 1.11(2) | 1.11(2) |
| C20–H20 | 1.08(2) | 1.09(2) | 1.10(2) | 1.08(2) |
| C21–H21 | 1.18(2) | 1.18(2) | 1.18(2) | 1.18(2) |
| C23–H23 | 1.08(2) | 1.07(2) | 1.07(3) | 1.08(2) |
| C24–H24 | 1.17(2) | 1.17(2) | 1.14(4) | 1.17(3) |
| C25–H25 | 1.09(2) | 1.09(2) | 1.07(2) | 1.09(2) |
| C26–H26 | 1.11(3) | 1.12(3) | 1.10(3) | 1.11(2) |
| C27–H27 | 1.11(2) | 1.11(2) | 1.08(3) | 1.11(2) |
| $\mathbf{C_{avr}}$ | 1.10(2) | 1.10(2) | 1.09(2) | 1.10(2) |

**Table S7** C–H bond lengths after HARs for the SP8 data.

| | rks-anh_nr | rhf-anh_rel | rks_rel | rks-anh_rel |
|---|---|---|---|---|
| C5–H5 | 1.09(2) | 1.09(2) | 1.10(2) | 1.09(2) |
| C6–H6 | 1.08(2) | 1.10(2) | 1.09(3) | 1.09(2) |
| C8–H8 | 1.04(2) | 1.05(2) | 1.11(2) | 1.05(2) |
| C9–H9 | 1.10(2) | 1.11(2) | 1.10(2) | 1.10(2) |
| C11–H11 | 1.10(2) | 1.10(2) | 1.09(3) | 1.10(2) |
| C12–H12 | 1.08(2) | 1.09(2) | 1.10(2) | 1.08(2) |
| C13–H13 | 1.03(2) | 1.04(2) | 1.12(2) | 1.03(2) |
| C14–H14 | 1.07(2) | 1.07(2) | 1.16(3) | 1.07(2) |
| C15–H15 | 1.08(2) | 1.09(2) | 1.13(3) | 1.08(2) |
| C17–H17 | 1.06(2) | 1.07(2) | 1.09(2) | 1.06(2) |
| C18–H18 | 1.08(3) | 1.08(3) | 1.08(2) | 1.08(3) |
| C19–H19 | 1.10(2) | 1.10(2) | 1.02(2) | 1.10(2) |
| C20–H20 | 1.08(2) | 1.10(2) | 1.08(2) | 1.09(2) |
| C21–H21 | 1.12(2) | 1.13(2) | 1.05(2) | 1.13(2) |
| C23–H23 | 1.08(2) | 1.08(2) | 1.07(2) | 1.08(2) |
| C24–H24 | 1.10(2) | 1.10(2) | 1.06(2) | 1.10(2) |
| C25–H25 | 1.16(2) | 1.16(2) | 1.06(3) | 1.16(2) |
| C26–H26 | 1.12(3) | 1.12(3) | 1.08(2) | 1.13(3) |
| C27–H27 | 1.11(2) | 1.12(2) | 1.09(2) | 1.11(2) |
| $\mathbf{C_{avr}}$ | 1.09(2) | 1.09(2) | 1.09(2) | 1.09(2) |

**Table S8** The minimum data resolution required (in $Å^{-1}$), according to the Kuhs equation (ref) and numbers of values of Gram–Charlier coefficients larger than 3 σ for anharmonic refinements.

| | **Ag data** | | | | | |
|---|---|---|---|---|---|---|
| | **rks-anh_nr** | | **rhf-anh_rel** | | **rks-anh_rel** | |
| | **res.** | **par.** | **res.** | **par.** | **res.** | **par.** |
| **exp.** | 0.83 | | 0.83 | | 0.83 | |
| **3rd** | 0.99 | 9 | 0.98 | 9 | 0.99 | 9 |
| **4th** | 1.14 | 13 | 1.13 | 12 | 1.14 | 13 |
| | **Mo data** | | | | | |
| | **rks-anh_nr** | | **rhf-anh_rel** | | **rks-anh_rel** | |
| | **res.** | **par.** | **res.** | **par.** | **res.** | **par.** |
| **exp.** | 1.00 | | 1.00 | | 1.00 | |
| **3rd** | 0.94 | 9 | 0.93 | 9 | 0.93 | 9 |
| **4th** | 1.08 | 15 | 1.07 | 15 | 1.08 | 15 |
| | **SP8 data** | | | | | |
| | **rks-anh_nr** | | **rhf-anh_rel** | | **rks-anh_rel** | |
| | **res.** | **par.** | **res.** | **par.** | **res.** | **par.** |
| **exp.** | 1.11 | | 1.11 | | 1.11 | |
| **3rd** | 1.01 | 9 | 1.00 | 9 | 1.01 | 9 |
| **4th** | 1.17 | 15 | 1.16 | 15 | 1.16 | 15 |

**Table S9** 3rd order of the Gram-Charlier coefficients obtained for the Ag data. Values higher than three standard uncertainties are highlighted in orange.

| | rks-anh_nr | rhf-anh_rel | rks-anh_rel |
|---|---|---|---|
| $U_{111}$ | 0.0000117(18) | 0.0000125(19) | 0.0000121(19) |
| $U_{222}$ | 0.000083(6) | 0.000096(6) | 0.000083(6) |
| $U_{333}$ | 0.0000083(10) | 0.0000086(10) | 0.0000087(10) |
| $U_{112}$ | 0.0000226(15) | 0.0000240(15) | 0.0000225(15) |
| $U_{113}$ | 0.0000054(8) | 0.0000057(8) | 0.0000057(8) |
| $U_{122}$ | 0.000045(2) | 0.000046(2) | 0.000046(2) |
| $U_{223}$ | 0.0000188(17) | 0.0000191(17) | 0.0000191(17) |
| $U_{133}$ | 0.0000041(6) | 0.0000044(6) | 0.0000043(6) |
| $U_{233}$ | 0.0000034(9) | 0.0000045(9) | 0.0000033(9) |
| $U_{123}$ | 0.0000012(8) | 0.0000012(8) | 0.0000012(8) |

**Table S10** 4th order of the Gram-Charlier coefficients obtained for the Ag data. Values higher than three standard uncertainties are highlighted in orange.

| | rks-anh_nr | rhf-anh_rel | rks-anh_rel |
|---|---|---|---|
| $U_{1111}$ | 0.0000036(10) | 0.0000094(10) | 0.0000076(10) |
| $U_{2222}$ | 0.000061(5) | 0.000089(5) | 0.000079(5) |
| $U_{3333}$ | 0.0000020(5) | 0.0000047(5) | 0.0000040(5) |
| $U_{1112}$ | 0.0000011(6) | 0.0000007(6) | 0.0000007(6) |
| $U_{1113}$ | 0.0000030(3) | 0.0000037(4) | 0.0000036(4) |
| $U_{1222}$ | 0.0000070(13) | 0.0000064(13) | 0.0000062(13) |
| $U_{2223}$ | 0.0000035(9) | 0.0000026(10) | 0.0000023(10) |
| $U_{1333}$ | 0.0000010(2) | 0.0000015(2) | 0.0000015(2) |
| $U_{2333}$ | 0.0000018(3) | 0.0000016(3) | 0.0000015(3) |
| $U_{1122}$ | 0.0000068(8) | 0.0000113(8) | 0.0000097(8) |
| $U_{1133}$ | 0.0000001(2) | 0.0000016(2) | 0.0000012(2) |
| $U_{2233}$ | 0.0000035(5) | 0.0000064(5) | 0.0000055(5) |
| $U_{1123}$ | 0.0000008(2) | 0.0000005(3) | 0.0000005(3) |
| $U_{1223}$ | 0.0000043(4) | 0.0000048(4) | 0.0000048(4) |
| $U_{1233}$ | 0.0000007(2) | 0.0000004(2) | 0.0000005(2) |

**Table S11** 3rd order of the Gram-Charlier coefficients obtained for the Mo data. Values higher than three standard uncertainties are highlighted in orange.

| | rks-anh_nr | rhf-anh_rel | rks-anh_rel |
|---|---|---|---|
| $U_{111}$ | -0.0000053(11) | -0.0000057(11) | -0.0000055(11) |
| $U_{222}$ | 0.000126(4) | 0.000135(4) | 0.000128(4) |
| $U_{333}$ | -0.0000037(6) | -0.0000039(6) | -0.0000039(6) |
| $U_{112}$ | 0.0000291(8) | 0.0000305(8) | 0.0000295(8) |
| $U_{113}$ | -0.0000025(4) | -0.0000027(4) | -0.0000026(4) |
| $U_{122}$ | -0.0000475(13) | -0.0000479(13) | -0.0000477(13) |
| $U_{223}$ | -0.0000219(10) | -0.0000220(10) | -0.0000219(10) |
| $U_{133}$ | -0.0000027(4) | -0.0000029(4) | -0.0000028(4) |
| $U_{233}$ | 0.0000073(5) | 0.0000081(5) | 0.0000075(5) |
| $U_{123}$ | 0.0000010(4) | 0.0000011(4) | 0.0000010(4) |

**Table S12** 4th order of the Gram-Charlier coefficients obtained for the Mo data. Values higher than three standard uncertainties are highlighted in orange.

| | rks-anh_nr | rhf-anh_rel | rks-anh_rel |
|---|---|---|---|
| $U_{1111}$ | 0.0000125(5) | 0.0000141(5) | 0.0000131(5) |
| $U_{2222}$ | 0.000066(2) | 0.000076(3) | 0.000070(2) |
| $U_{3333}$ | 0.0000077(2) | 0.0000084(2) | 0.0000079(2) |
| $U_{1112}$ | -0.0000020(3) | -0.0000020(3) | -0.0000018(3) |
| $U_{1113}$ | 0.00000304(17) | 0.00000324(17) | 0.00000319(17) |
| $U_{1222}$ | -0.0000076(7) | -0.0000077(7) | -0.0000073(7) |
| $U_{2223}$ | -0.0000060(5) | -0.0000057(5) | -0.0000056(5) |
| $U_{1333}$ | 0.00000159(12) | 0.00000173(12) | 0.00000170(12) |
| $U_{2333}$ | -0.00000078(15) | -0.00000067(15) | -0.00000062(15) |
| $U_{1122}$ | 0.0000094(3) | 0.0000108(4) | 0.0000100(4) |
| $U_{1133}$ | 0.00000316(11) | 0.00000355(11) | 0.00000331(11) |
| $U_{2233}$ | 0.0000062(2) | 0.0000071(2) | 0.0000065(2) |
| $U_{1123}$ | -0.00000072(12) | -0.00000059(12) | -0.00000060(12) |
| $U_{1223}$ | 0.00000315(18) | 0.00000330(18) | 0.00000325(18) |
| $U_{1233}$ | -0.00000061(10) | -0.00000050(10) | -0.00000051(10) |

**Table S13** 3rd order of the Gram-Charlier coefficients obtained for the SP8 data. Values higher than three standard uncertainties are highlighted in orange.

| | rks-anh_nr | rhf-anh_rel | rks-anh_rel |
|---|---|---|---|
| $U_{111}$ | -0.0000023(8) | -0.0000029(8) | -0.0000025(8) |
| $U_{222}$ | 0.000069(4) | 0.000079(4) | 0.000072(4) |
| $U_{333}$ | -0.0000072(5) | -0.0000074(5) | -0.0000073(5) |
| $U_{112}$ | 0.0000169(7) | 0.0000182(7) | 0.0000172(7) |
| $U_{113}$ | -0.0000022(4) | -0.0000023(4) | -0.0000023(4) |
| $U_{122}$ | -0.0000270(11) | -0.0000275(11) | -0.0000271(11) |
| $U_{223}$ | -0.0000148(9) | -0.0000151(9) | -0.0000148(9) |
| $U_{133}$ | -0.0000022(3) | -0.0000024(3) | -0.0000023(3) |
| $U_{233}$ | 0.0000052(5) | 0.0000060(5) | 0.0000054(5) |
| $U_{123}$ | 0.0000005(4) | 0.0000005(4) | 0.0000005(4) |

**Table S14** 4th order of the Gram-Charlier coefficients obtained for the SP8 data. Values higher than three standard uncertainties are highlighted in orange.

| | rks-anh_nr | rhf-anh_rel | rks-anh_rel |
|---|---|---|---|
| $U_{1111}$ | 0.0000041(4) | 0.0000045(4) | 0.0000036(4) |
| $U_{2222}$ | 0.000010(2) | 0.000014(2) | 0.0000096(19) |
| $U_{3333}$ | 0.00000185(18) | 0.00000196(18) | 0.00000162(18) |
| $U_{1112}$ | -0.00000166(19) | -0.00000160(19) | -0.00000152(19) |
| $U_{1113}$ | 0.00000070(14) | 0.00000066(14) | 0.00000065(14) |
| $U_{1222}$ | -0.0000054(5) | -0.0000053(5) | -0.0000051(5) |
| $U_{2223}$ | -0.0000029(4) | -0.0000028(4) | -0.0000027(4) |
| $U_{1333}$ | 0.00000080(9) | 0.00000078(9) | 0.00000077(9) |
| $U_{2333}$ | -0.00000087(11) | -0.00000081(11) | -0.00000078(11) |
| $U_{1122}$ | 0.0000024(3) | 0.0000029(3) | 0.0000022(3) |
| $U_{1133}$ | 0.00000069(9) | 0.00000077(9) | 0.00000059(9) |
| $U_{2233}$ | 0.00000114(19) | 0.00000143(19) | 0.00000100(19) |
| $U_{1123}$ | -0.00000042(9) | -0.00000035(9) | -0.00000035(9) |
| $U_{1223}$ | 0.00000209(15) | 0.00000208(15) | 0.00000205(15) |
| $U_{1233}$ | -0.00000039(7) | -0.00000033(7) | -0.00000033(7) |


**Figure S2** Plot of the numeric values of the 4$^{th}$ order G-C coefficients within three e.s.d.'s for Ag, Mo and SP8 data at different level of theory.

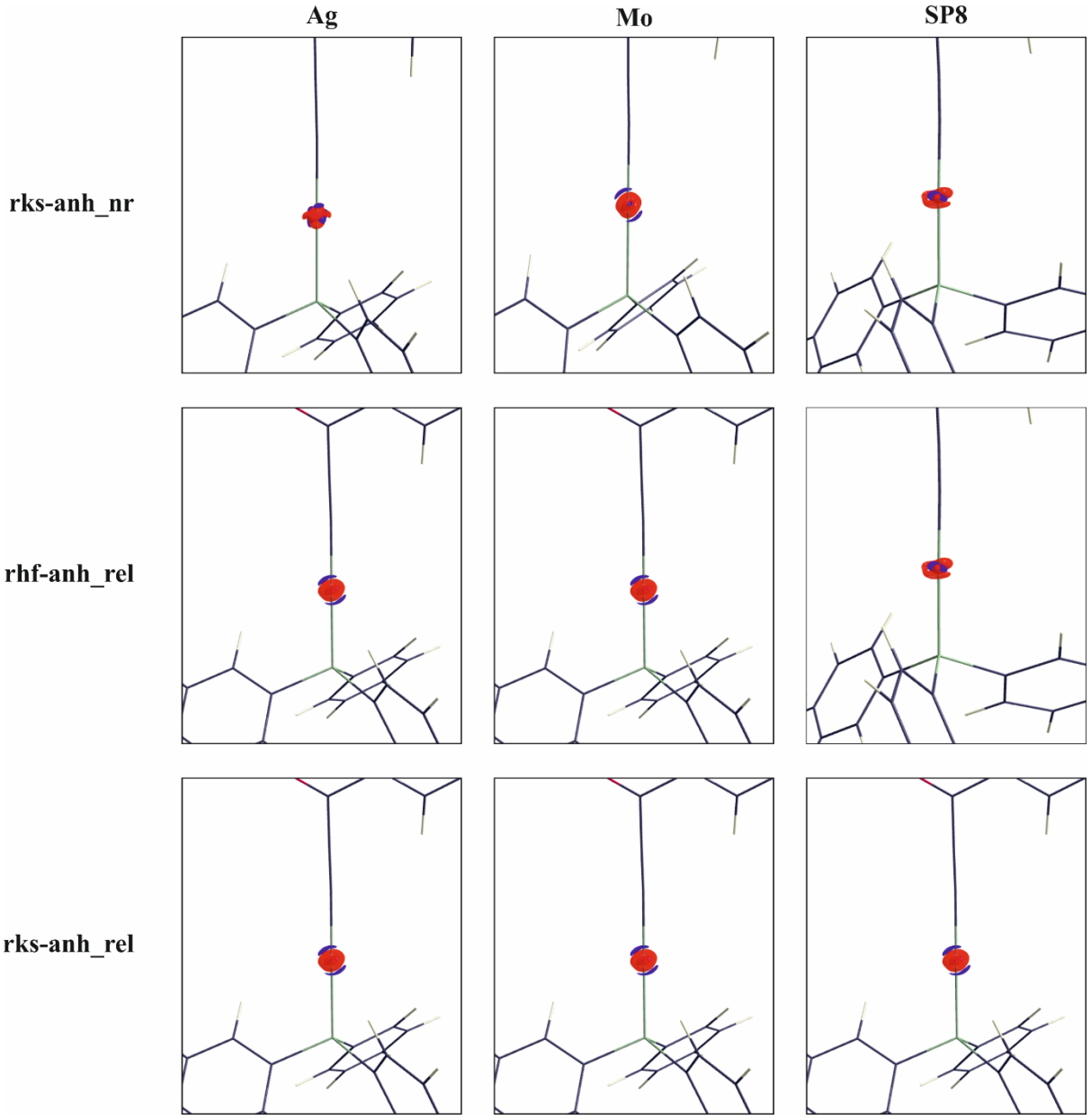


**Figure S3** Graphical representation of the probability function of 3rd and 4th order of the Gram–Charlier coefficients of gold at the 50 % probability level for all considered anharmonic refinements.

**Table S15** The difference between ADPs obtained from rks_nr, rhf_rel and rks_rel, representing effect of electron correlation (rks_rel – rhf_rel) and relativity (rks_rel – rks_nr)for Ag and Mo data.

| Ag data | | | | | |
|---|---|---|---|---|---|
| Au | rks_nr | rhf_rel | rks_rel | ECORR | REL |
| $U_{11}$ | 0.01630(2) | 0.01646(2) | 0.01662(2) | 0.00016 | 0.00032 |
| $U_{22}$ | 0.02220(2) | 0.02238(2) | 0.02251(2) | 0.00013 | 0.00031 |
| $U_{33}$ | 0.01289(2) | 0.01303(2) | 0.01318(2) | 0.00015 | 0.00030 |
| $U_{12}$ | 0.00383(1) | 0.00383(1) | 0.00382(1) | -0.00001 | -0.00001 |
| $U_{13}$ | 0.00197(1) | 0.00198(1) | 0.00120(1) | 0.00002 | 0.00002 |
| $U_{23}$ | 0.00323(1) | 0.00323(1) | 0.00322(1) | -0.00001 | -0.00001 |
| | | | **Mo data** | | |
| **Au** | **rks_nr** | **rhf_rel** | **rks_rel** | **ECORR** | **REL** |
| U11 | 0.01786(1) | 0.01799(1) | 0.01810(1) | 0.00011 | 0.00024 |
| U22 | 0.02396(2) | 0.02411(2) | 0.02422(2) | 0.00011 | 0.00025 |
| U33 | 0.01349(1) | 0.01362(1) | 0.01372(1) | 0.00010 | 0.00023 |
| U12 | -0.004305(8) | -0.004307(8) | -0.004301(8) | 0.00001 | 0.00000 |
| U13 | 0.001988(8) | 0.001992(8) | 0.002005(8) | 0.00001 | 0.00002 |
| U23 | -0.003720(7) | -0.003721(7) | -0.003715(8) | 0.00001 | 0.00001 |

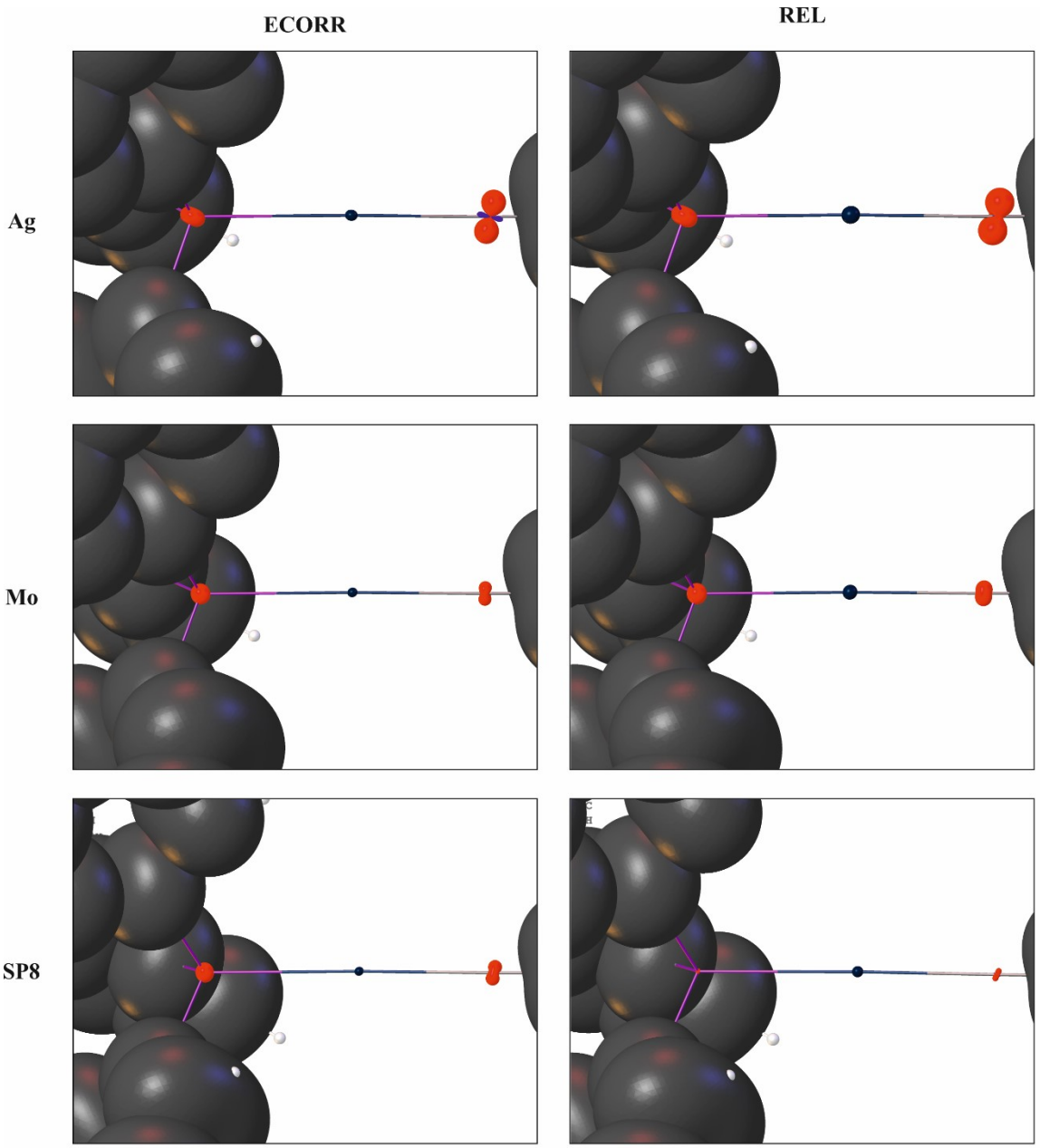


**Figure S4** Graphical representation of the differences between ADPs obtained from rks_nr, rhf_rel and rks_rel, for Ag, Mo and SP8 data in the P–Au–C direction. The central atom is Au, left P and right C.

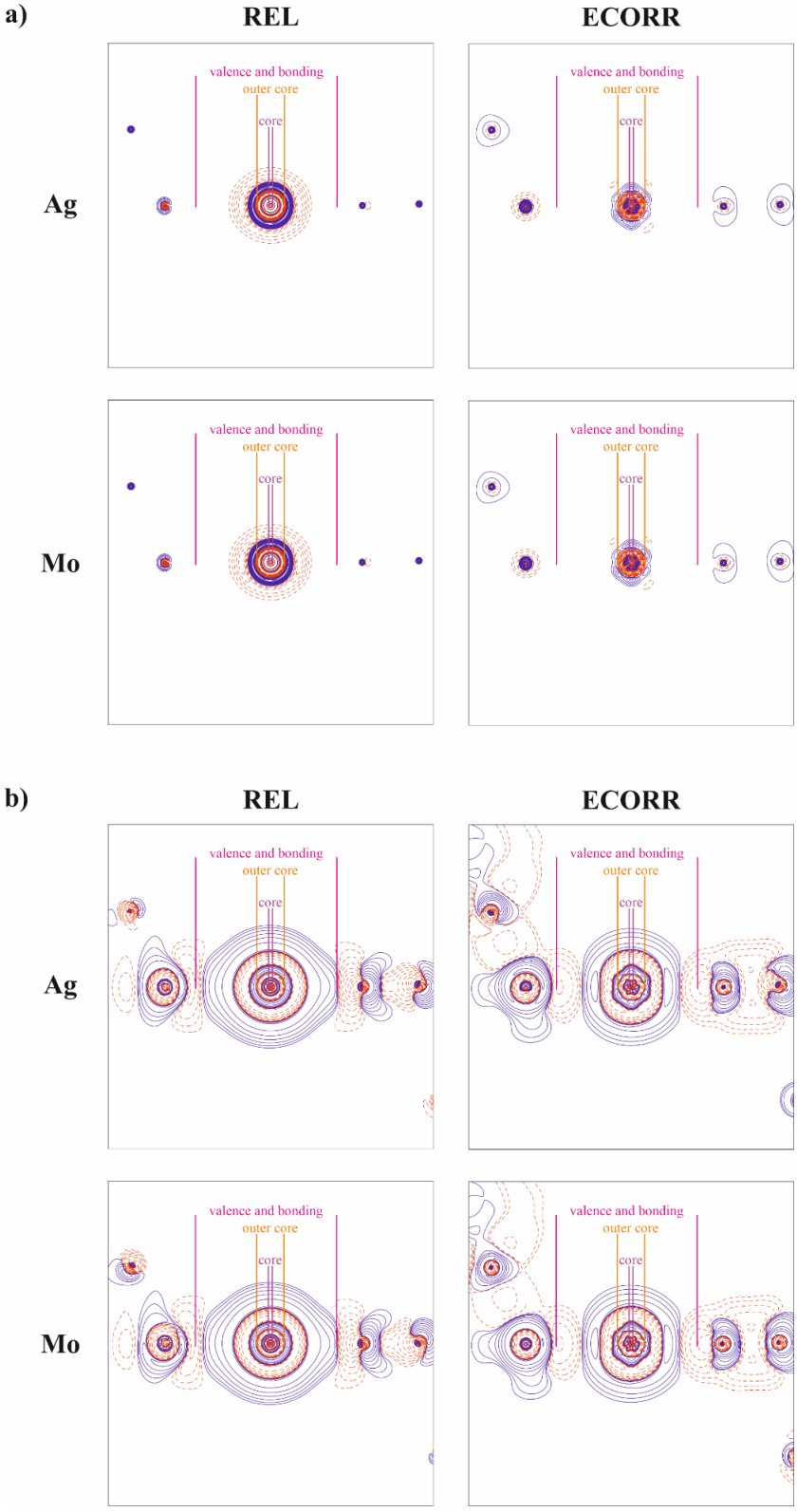


**Figure S5** Difference maps of (a) the static electron density (contour ±0.01 e A−3) and (b) negative Laplacian (contour values in geometric order, starting value ±0.1, increments 2) in the plane of P–Au–C atoms exposing the effects of relativity (REL) and electron correlation (ECORR) for Ag and Mo data. Values of the positive and negative difference densities are denoted by the blue, solid and red, dashed lines, respectively.

**Table S16** **Selected BCP topological properties of** Au–C bond resulting from HAR performed against Ag and Mo data. "dev" represents changes in ρ(r) and ∇2ρ(r) arising from REL, ECORR and ANH and are expressed in percentages.

| | **Ag data** | | | | | | | | | | |
|---|---|---|---|---|---|---|---|---|---|---|---|
| | **ρ(r)** | **dev** | **$\nabla^2\rho(r)$** | **dev** | **$V_r$** | **$G_r$** | **$H_r$** | **$\lvert V_r\rvert/G_r$** | **ε** | **$r_{Au\text{-}BCP}$** | **$r_{Au\text{-}P}$** |
| | **eÅ$^{-3}$** | **%** | **eÅ$^{-5}$** | **%** | **[Haa$_0^{-3}$]** | **[Haa$_0^{-3}$]** | **[Haa$_0^{-3}$]** | | | **[Å]** | **[Å]** |
| **rks-anh_nr** | 0.930 | -2.1 | 8.389 | 12.0 | -0.1943 | 0.1407 | -0.0536 | 1.38 | 0.02 | 1.09 | 1.9878(8) |
| **rhf-anh_rel** | 0.972 | 2.3 | 8.291 | 10.7 | -0.2133 | 0.1497 | -0.0637 | 1.43 | 0.00 | 1.06 | 1.9886(10) |
| **rks-rel** | 0.971 | 2.2 | 6.902 | -7.9 | -0.1950 | 0.1333 | -0.0617 | 1.46 | 0.02 | 1.07 | 1.9892(10) |
| **rks-anh_rel** | 0.950 | | 7.491 | | -0.1964 | 0.1371 | -0.0593 | 1.43 | 0.01 | 1.06 | 1.9884(10) |
| | Mo data | | | | | | | | | | |
| | ρ(r) | dev | **$\nabla^2\rho(r)$** | dev | $V_r$ | $G_r$ | $H_r$ | $\lvert V_r\rvert/G_r$ | ε | $r_{Au\text{-}BCP}$ | $r_{Au\text{-}P}$ |
| | eÅ$^{-3}$ | % | eÅ$^{-5}$ | % | [Haa$_0^{-3}$] | [Haa$_0^{-3}$] | [Haa$_0^{-3}$] | | | [Å] | [Å] |
| **rks-anh_nr** | 0.932 | -2.5 | 9.007 | 19.5 | -0.1977 | 0.1456 | -0.0521 | 1.36 | 0.00 | 1.07 | 1.9854(7) |
| **rhf-anh_rel** | 0.978 | 2.3 | 8.341 | 10.7 | -0.2151 | 0.1508 | -0.0643 | 1.43 | 0.00 | 1.05 | 1.9856(7) |
| **rks-rel** | 0.976 | 2.1 | 6.974 | -7.5 | -0.1969 | 0.1346 | -0.0623 | 1.46 | 0.02 | 1.07 | 1.9851(9) |
| **rks-anh_rel** | 0.956 | | 7.537 | | -0.1983 | 0.1382 | -0.0600 | 1.43 | 0.01 | 1.06 | 1.9854(7) |

**Table S17** Selected BCP topological properties of Au–P bond resulting from HAR performed against Ag and Mo data. "dev" represents changes in ρ(r) and $\nabla^2\rho(r)$ arising from REL, ECORR and ANH and are expressed in percentages.

| | **Ag data** | | | | | | | | | | |
|---|---|---|---|---|---|---|---|---|---|---|---|
| | **ρ(r)** | **dev** | **$\nabla^2\rho(r)$** | **dev** | **$V_r$** | **$G_r$** | **$H_r$** | **$\lvert V_r\rvert/G_r$** | **ε** | **$r_{Au\text{-}BCP}$** | **$r_{Au\text{-}P}$** |
| | **eÅ$^{-3}$** | **%** | **eÅ$^{-5}$** | **%** | **[Haa$_0^{-3}$]** | **[Haa$_0^{-3}$]** | **[Haa$_0^{-3}$]** | | | **[Å]** | **[Å]** |
| **rks-anh_nr** | 0.739 | -5.1 | 0.728 | -9.7 | -0.1170 | 0.0623 | -0.0547 | 1.88 | 0.00 | 1.20 | 2.2742(2) |
| **rhf-anh_rel** | 0.786 | 0.9 | 1.399 | 73.6 | -0.1319 | 0.0732 | -0.0587 | 1.80 | 0.01 | 1.16 | 2.2741(2) |
| **rks-rel** | 0.803 | 3.1 | 2.237 | 177.5 | -0.1381 | 0.0806 | -0.0574 | 1.71 | 0.04 | 1.15 | 2.2733(3) |
| **rks-anh_rel** | 0.779 | | 0.806 | | -0.1244 | 0.0664 | -0.0580 | 1.87 | 0.01 | 1.17 | 2.2742(2) |
| | **Mo data** | | | | | | | | | | |
| | **ρ(r)** | **dev** | **$\nabla^2\rho(r)$** | **dev** | **$V_r$** | **$G_r$** | **$H_r$** | **$\lvert V_r\rvert/G_r$** | **ε** | **$r_{Au\text{-}BCP}$** | **$r_{Au\text{-}P}$** |
| | **eÅ$^{-3}$** | **%** | **eÅ$^{-5}$** | **%** | **[Haa$_0^{-3}$]** | **[Haa$_0^{-3}$]** | **[Haa$_0^{-3}$]** | | | **[Å]** | **[Å]** |
| **rks-anh_nr** | 0.740 | -5.1 | 0.744 | -11.8 | -0.1175 | 0.0626 | -0.0549 | 1.88 | 0.00 | 1.20 | 2.2726(2) |
| **rhf-anh_rel** | 0.788 | 1.0 | 1.431 | 69.5 | -0.1326 | 0.0737 | -0.0589 | 1.80 | 0.01 | 1.16 | 2.2726(2) |
| **rks-rel** | 0.805 | 3.2 | 2.230 | 164.2 | -0.1384 | 0.0808 | -0.0576 | 1.71 | 0.05 | 1.15 | 2.2725(2) |
| **rks-anh_rel** | 0.780 | | 0.844 | | -0.1250 | 0.0669 | -0.0581 | 1.87 | 0.01 | 1.17 | 2.2726(2) |

**Table S18** AIM charges resulting from HARs performed against Ag data.

| atom | rks-anh_nr | rhf-anh_rel | rks_rel | rks-anh_rel |
|---|---|---|---|---|
| Au1 | 1.041 | 0.452 | 0.184 | 0.618 |
| P1 | 2.231 | 2.448 | 1.992 | 2.120 |
| Cl1 | -0.252 | -0.326 | 0.146 | -0.250 |
| O1 | -1.140 | -1.321 | -0.962 | -1.138 |
| C1 | -0.161 | -0.092 | -0.034 | -0.170 |
| C2 | 1.029 | -0.509 | -0.124 | -0.332 |
| C3 | -0.042 | 1.224 | 1.026 | 1.030 |
| C4 | 0.004 | -0.053 | 0.370 | -0.044 |
| C5 | 0.054 | 0.001 | 0.064 | 0.003 |
| C6 | 0.080 | 0.077 | 0.165 | 0.054 |
| C7 | 0.045 | 0.086 | 0.402 | 0.079 |
| C8 | 0.078 | 0.071 | 0.173 | 0.043 |
| C9 | -0.592 | 0.107 | 0.093 | 0.079 |
| C10 | 0.092 | -0.690 | -0.662 | -0.594 |
| C11 | 0.028 | 0.122 | 0.023 | 0.096 |
| C12 | 0.118 | 0.034 | 0.054 | 0.024 |
| C13 | 0.095 | 0.162 | 0.078 | 0.120 |
| C14 | 0.048 | 0.158 | 0.037 | 0.108 |
| C15 | -0.595 | 0.036 | 0.018 | 0.033 |
| C16 | 0.078 | -0.692 | -0.654 | -0.589 |
| C17 | 0.006 | 0.080 | 0.057 | 0.072 |
| C18 | 0.021 | 0.010 | 0.021 | 0.008 |
| C19 | -0.369 | 0.041 | 0.043 | 0.021 |
| C20 | -0.008 | -0.012 | 0.014 | -0.010 |
| C21 | 0.040 | 0.047 | -0.007 | 0.037 |
| C22 | -0.491 | -0.429 | -0.646 | -0.350 |
| C23 | 0.128 | 0.220 | 0.007 | 0.228 |

| | | | | |
|---|---|---|---|---|
| C24 | 0.002 | 0.005 | 0.017 | -0.009 |
| C25 | 0.205 | 0.383 | 0.015 | 0.346 |
| C26 | 0.093 | 0.232 | 0.006 | 0.218 |
| C27 | 0.037 | 0.006 | -0.001 | 0.004 |
| H5 | 0.028 | 0.043 | 0.031 | 0.030 |
| H6 | 0.051 | 0.069 | 0.028 | 0.055 |
| H8 | 0.011 | 0.012 | 0.012 | 0.012 |
| H9 | -0.019 | -0.027 | -0.007 | -0.019 |
| H11 | -0.009 | -0.004 | -0.004 | 0.001 |
| H12 | -0.040 | -0.055 | -0.002 | -0.040 |
| H13 | 0.023 | 0.020 | -0.011 | 0.024 |
| H14 | -0.039 | -0.061 | -0.045 | -0.036 |
| H15 | -0.021 | -0.026 | -0.009 | -0.021 |
| H17 | 0.007 | 0.022 | 0.002 | 0.018 |
| H18 | 0.007 | 0.010 | 0.007 | 0.008 |
| H19 | -0.002 | -0.008 | 0.010 | -0.003 |
| H20 | 0.020 | 0.024 | 0.000 | 0.022 |
| H21 | 0.010 | 0.016 | 0.002 | 0.012 |
| H23 | -0.024 | -0.030 | 0.018 | -0.020 |
| H24 | 0.011 | 0.011 | 0.017 | 0.011 |
| H25 | 0.051 | 0.067 | 0.023 | 0.054 |
| H26 | 0.019 | 0.018 | -0.003 | 0.023 |
| H27 | 0.010 | 0.017 | 0.017 | 0.012 |

**Table S19** AIM charges resulting from HARs performed against Mo data.

| atom | rks-anh_nr | rhf-anh_rel | rks_rel | rks-anh_rel |
|---|---|---|---|---|
| Au1 | 1.021 | 0.445 | 0.191 | 0.591 |
| P1 | 2.234 | 2.448 | 1.995 | 2.122 |
| Cl1 | -0.251 | -0.324 | 0.151 | -0.249 |
| O1 | -1.141 | -1.324 | -0.988 | -1.139 |
| C1 | -0.163 | -0.090 | -0.027 | -0.168 |
| C2 | -0.370 | -0.510 | -0.122 | -0.332 |
| C3 | 1.024 | 1.222 | 1.027 | 1.026 |
| C4 | -0.041 | -0.052 | 0.365 | -0.042 |
| C5 | 0.008 | 0.009 | 0.055 | 0.006 |
| C6 | 0.039 | 0.055 | 0.182 | 0.039 |
| C7 | 0.086 | 0.093 | 0.401 | 0.085 |
| C8 | 0.044 | 0.068 | 0.167 | 0.044 |
| C9 | 0.033 | 0.039 | 0.106 | 0.032 |
| C10 | -0.595 | -0.700 | -0.666 | -0.600 |
| C11 | 0.067 | 0.077 | 0.005 | 0.067 |
| C12 | 0.055 | 0.077 | 0.065 | 0.055 |
| C13 | 0.083 | 0.101 | 0.026 | 0.083 |
| C14 | 0.073 | 0.118 | 0.039 | 0.083 |
| C15 | 0.051 | 0.039 | 0.028 | 0.038 |
| C16 | -0.590 | -0.686 | -0.660 | -0.587 |
| C17 | 0.078 | 0.077 | 0.065 | 0.072 |
| C18 | 0.023 | 0.044 | 0.051 | 0.025 |
| C19 | 0.021 | 0.032 | 0.026 | 0.021 |
| C20 | 0.012 | 0.011 | 0.026 | 0.007 |
| C21 | 0.013 | 0.009 | -0.009 | 0.010 |
| C22 | -0.477 | -0.413 | -0.651 | -0.337 |
| C23 | 0.142 | 0.245 | 0.045 | 0.250 |

| | | | | |
|---|---|---|---|---|
| C24 | 0.002 | 0.003 | 0.030 | -0.007 |
| C25 | 0.234 | 0.418 | 0.047 | 0.370 |
| C26 | 0.103 | 0.248 | 0.028 | 0.241 |
| C27 | 0.046 | 0.018 | 0.027 | 0.012 |
| H5 | 0.030 | 0.043 | 0.030 | 0.031 |
| H6 | 0.063 | 0.085 | 0.020 | 0.067 |
| H8 | 0.015 | 0.020 | 0.014 | 0.016 |
| H9 | 0.015 | 0.027 | -0.010 | 0.016 |
| H11 | 0.005 | 0.017 | 0.006 | 0.015 |
| H12 | -0.053 | -0.079 | -0.004 | -0.056 |
| H13 | 0.051 | 0.066 | 0.032 | 0.052 |
| H14 | -0.018 | -0.029 | -0.040 | -0.016 |
| H15 | -0.024 | -0.026 | -0.018 | -0.025 |
| H17 | 0.006 | 0.020 | -0.010 | 0.016 |
| H18 | -0.007 | -0.011 | -0.016 | -0.007 |
| H19 | -0.005 | -0.010 | 0.020 | -0.007 |
| H20 | 0.010 | 0.012 | 0.000 | 0.012 |
| H21 | 0.024 | 0.035 | 0.000 | 0.026 |
| H23 | -0.030 | -0.041 | -0.010 | -0.027 |
| H24 | 0.007 | 0.006 | 0.000 | 0.008 |
| H25 | 0.030 | 0.040 | -0.004 | 0.034 |
| H26 | 0.015 | 0.015 | -0.025 | 0.018 |
| H27 | 0.004 | 0.009 | -0.007 | 0.005 |

**Table S20** AIM charges resulting from HARs performed against SP8 data.

| atom | rks-anh_nr | rhf-anh_rel | rks_rel | rks-anh_rel |
|---|---|---|---|---|
| Au1 | 0.994 | 0.430 | 0.189 | 0.557 |
| P1 | 2.223 | 2.436 | 1.986 | 2.110 |
| Cl1 | -0.252 | -0.325 | 0.142 | -0.250 |
| O1 | -1.137 | -1.320 | -0.975 | -1.134 |
| C1 | -0.168 | -0.094 | -0.037 | -0.170 |
| C2 | -0.368 | -0.505 | -0.127 | -0.328 |
| C3 | 1.019 | 1.217 | 1.023 | 1.022 |
| C4 | -0.041 | -0.053 | 0.372 | -0.043 |
| C5 | 0.018 | 0.026 | 0.078 | 0.017 |
| C6 | 0.053 | 0.071 | 0.185 | 0.052 |
| C7 | 0.078 | 0.083 | 0.403 | 0.078 |
| C8 | 0.058 | 0.081 | 0.185 | 0.056 |
| C9 | 0.024 | 0.025 | 0.082 | 0.023 |
| C10 | -0.587 | -0.697 | -0.657 | -0.596 |
| C11 | 0.080 | 0.096 | 0.023 | 0.079 |
| C12 | 0.034 | 0.041 | 0.035 | 0.033 |
| C13 | 0.115 | 0.135 | 0.060 | 0.112 |
| C14 | 0.054 | 0.086 | 0.019 | 0.061 |
| C15 | 0.049 | 0.037 | 0.016 | 0.036 |
| C16 | -0.589 | -0.691 | -0.661 | -0.587 |
| C17 | 0.063 | 0.061 | 0.048 | 0.057 |
| C18 | 0.030 | 0.047 | 0.069 | 0.031 |
| C19 | 0.021 | 0.036 | 0.031 | 0.020 |
| C20 | 0.006 | -0.001 | 0.031 | 0.000 |
| C21 | 0.030 | 0.029 | 0.012 | 0.026 |
| C22 | -0.470 | -0.413 | -0.650 | -0.328 |
| C23 | 0.155 | 0.274 | 0.045 | 0.273 |

| | | | | |
|---|---|---|---|---|
| C24 | 0.034 | 0.039 | 0.054 | 0.022 |
| C25 | 0.216 | 0.378 | 0.010 | 0.352 |
| C26 | 0.107 | 0.274 | 0.019 | 0.254 |
| C27 | 0.042 | -0.003 | 0.014 | 0.004 |
| H5 | 0.024 | 0.032 | 0.023 | 0.024 |
| H6 | 0.053 | 0.076 | 0.013 | 0.057 |
| H8 | 0.007 | 0.013 | 0.006 | 0.007 |
| H9 | 0.021 | 0.037 | 0.002 | 0.021 |
| H11 | -0.001 | 0.006 | -0.001 | 0.009 |
| H12 | -0.047 | -0.064 | 0.011 | -0.048 |
| H13 | 0.021 | 0.030 | 0.004 | 0.022 |
| H14 | -0.009 | -0.012 | -0.030 | -0.006 |
| H15 | -0.017 | -0.016 | -0.005 | -0.018 |
| H17 | 0.016 | 0.033 | 0.001 | 0.027 |
| H18 | -0.003 | -0.007 | -0.024 | -0.003 |
| H19 | -0.007 | -0.011 | 0.012 | -0.008 |
| H20 | 0.011 | 0.014 | -0.006 | 0.014 |
| H21 | 0.015 | 0.024 | -0.012 | 0.017 |
| H23 | -0.033 | -0.039 | -0.009 | -0.029 |
| H24 | -0.007 | -0.014 | -0.011 | -0.008 |
| H25 | 0.046 | 0.065 | 0.019 | 0.052 |
| H26 | 0.019 | 0.019 | -0.021 | 0.021 |
| H27 | 0.004 | 0.012 | 0.002 | 0.006 |

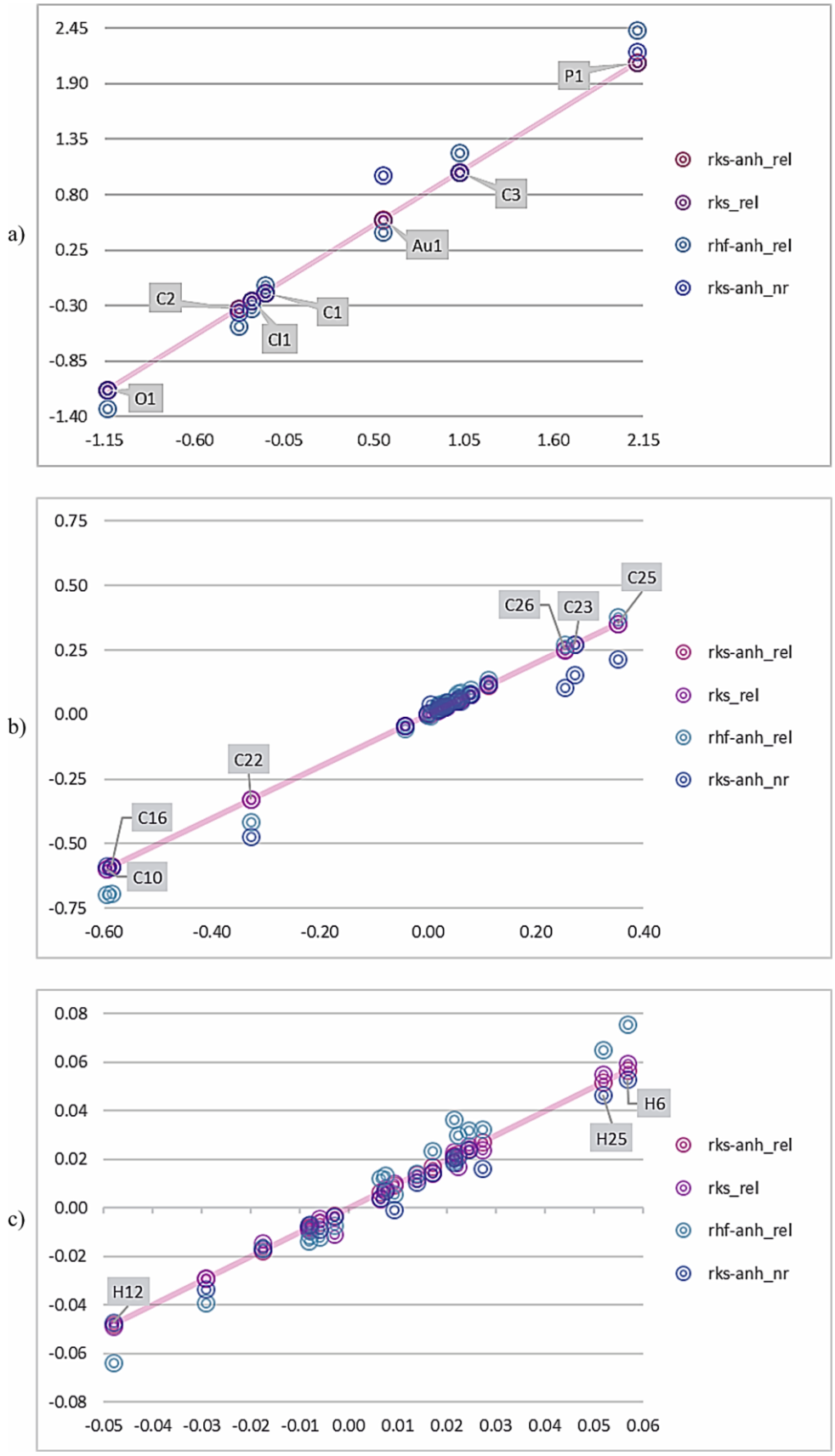


**Figure S6** Plot of atomic charges obtained from QTAIM analysis after HARs against SP8 data showing changes arising from ANH, REL and ECORR. Pink line represents y=x plot.

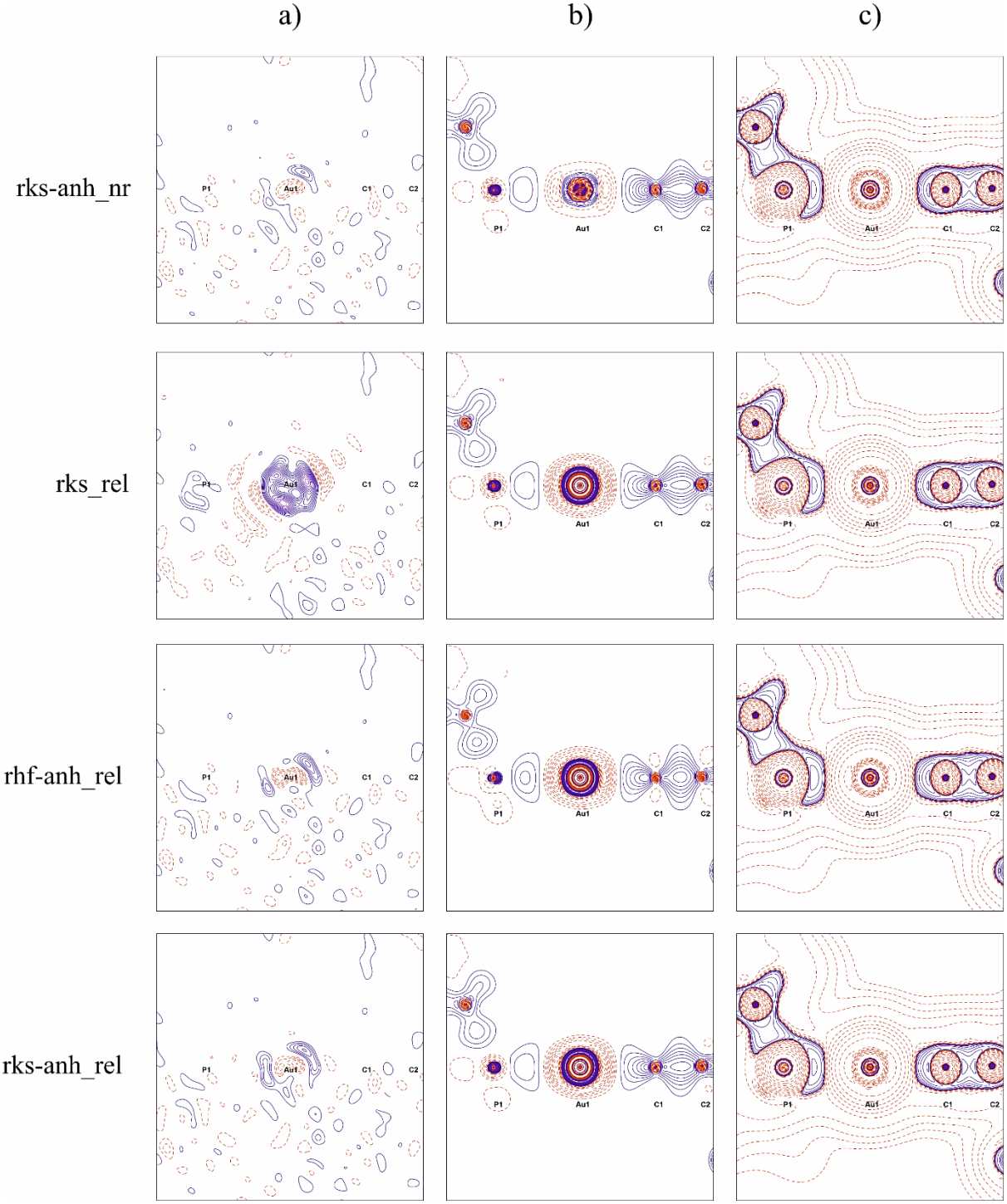


**Figure S7** (a) Residual density, (b) deformation density and (c) negative Laplacian maps resulting from HAR performed against Ag data. Contour level: 0.1eÅ$^{-3}$ (a and b) and 0.1eÅ$^{-3}$ (c). Colours: blue – positive, red – negative.

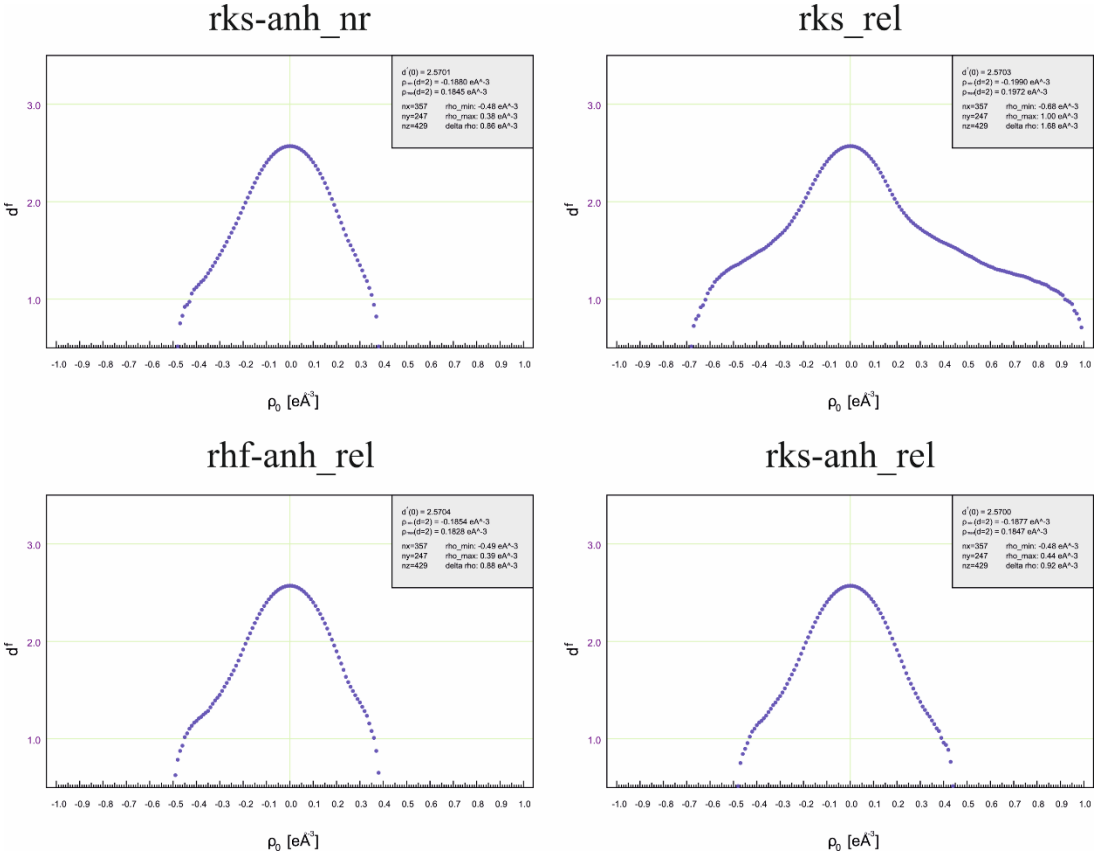


**Figure S8** The fractal dimension plots of the residual electron density resulting from HAR performed against Ag data.

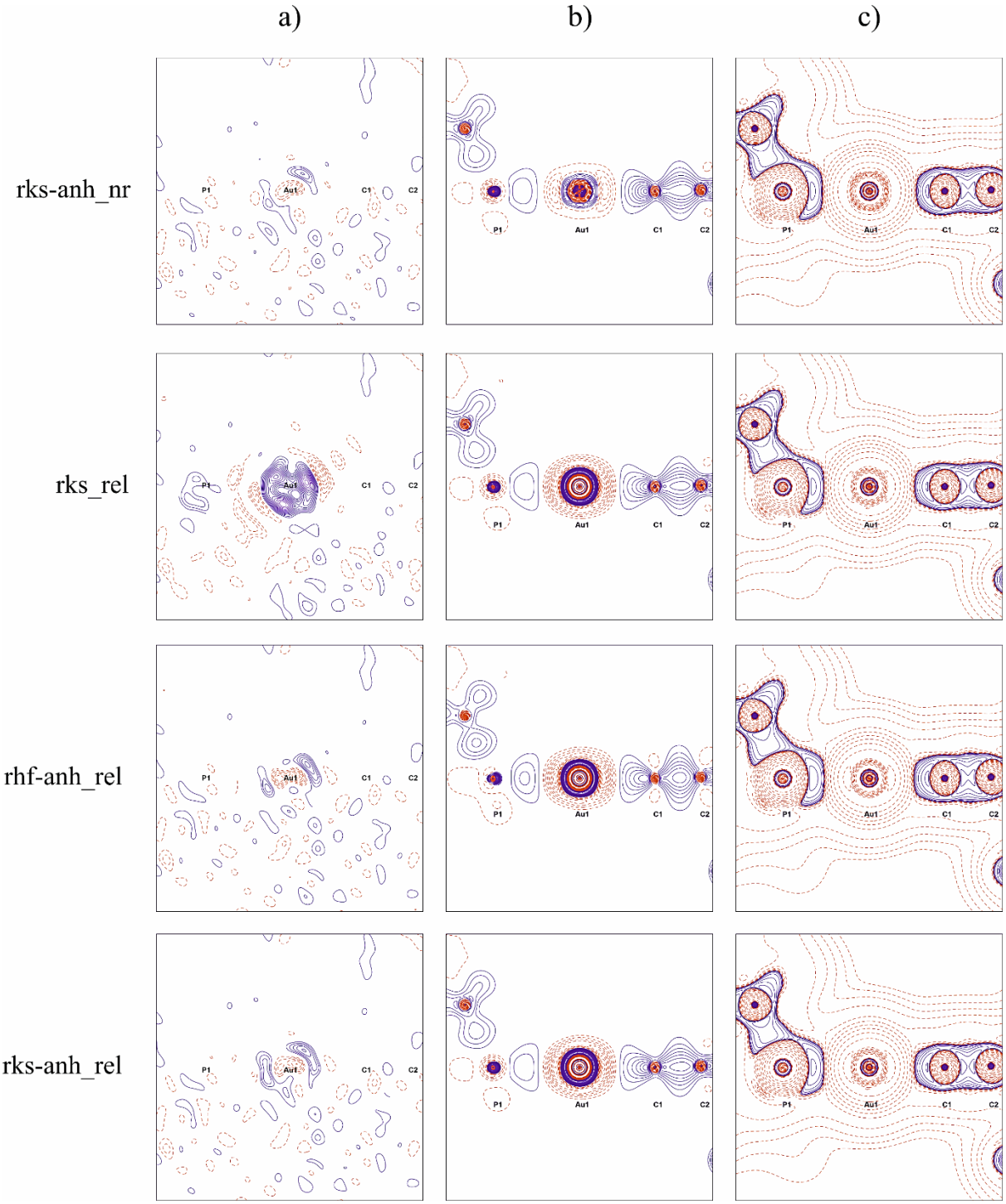


**Figure S9** (a) Residual density, (b) deformation density and (c) negative Laplacian maps resulting from HAR performed against Mo data. Contour level: 0.1eÅ$^{-3}$ (a and b) and 0.1eÅ$^{-3}$ (c). Colours: blue – positive, red – negative.

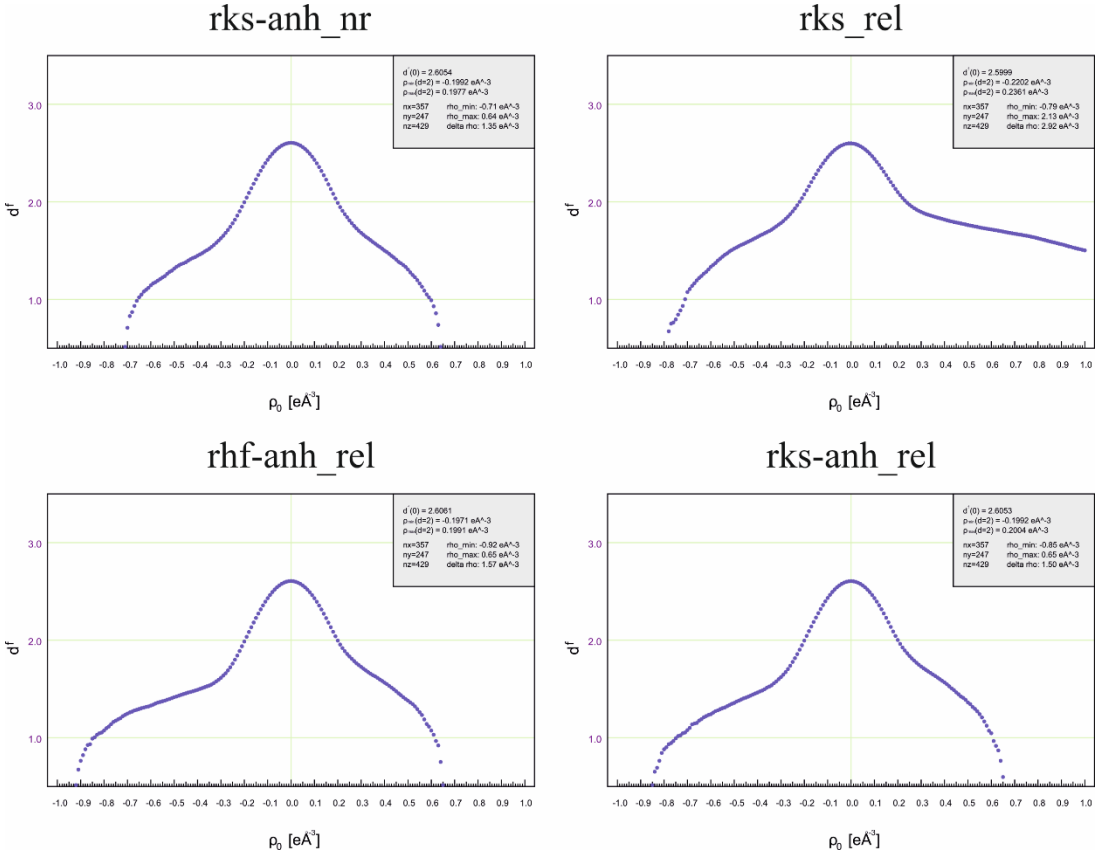


**Figure S10**The fractal dimension plots of the residual electron density for resulting from HAR performed against Mo data.

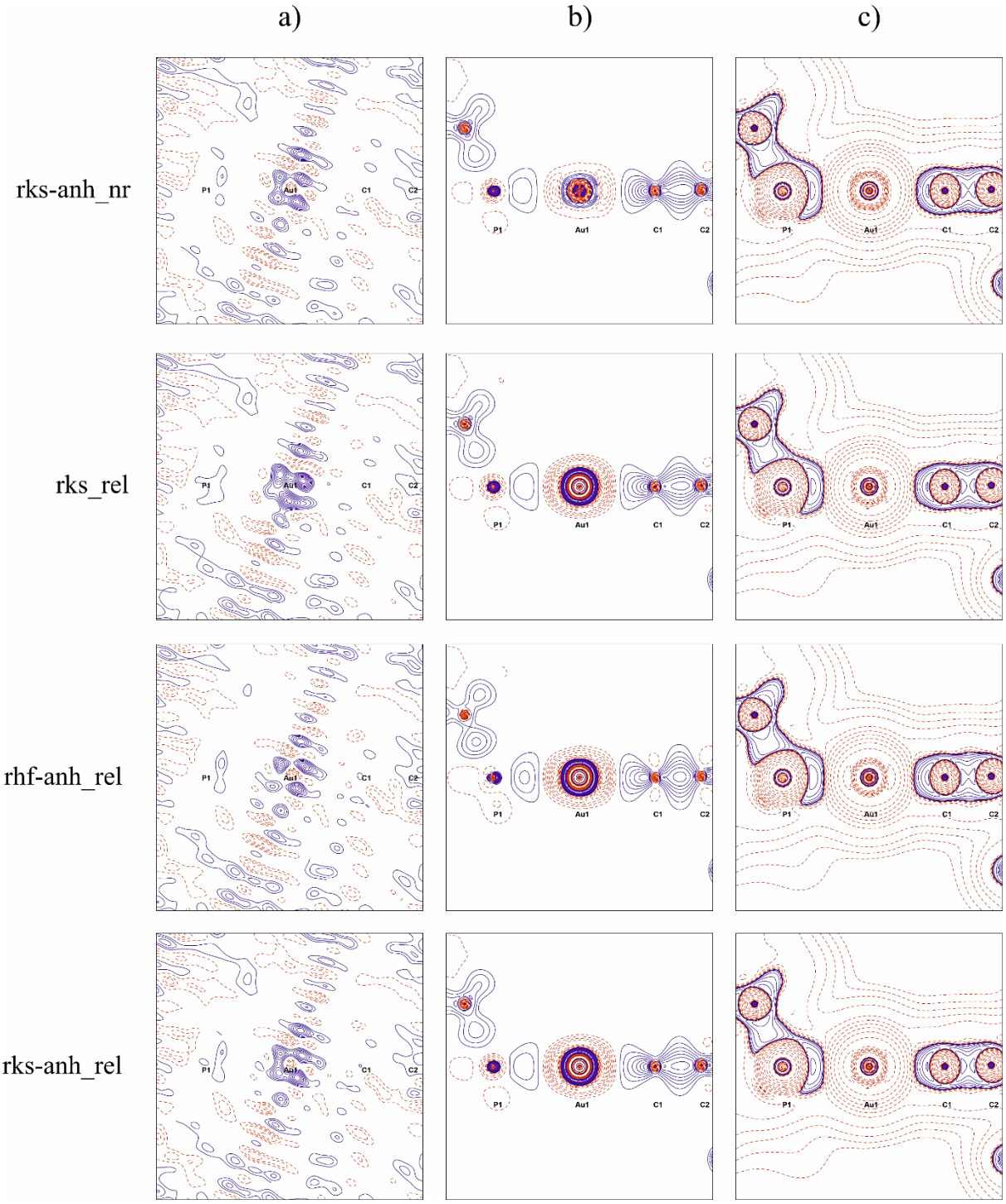


**Figure S11**(a) Residual density, (b) deformation density and (c) negative Laplacian maps resulting from HAR performed against SP8 data. Contour level: 0.1eÅ$^{-3}$ (a and b) and 0.1eÅ$^{-3}$ (c). Colours: blue – positive, red – negative.

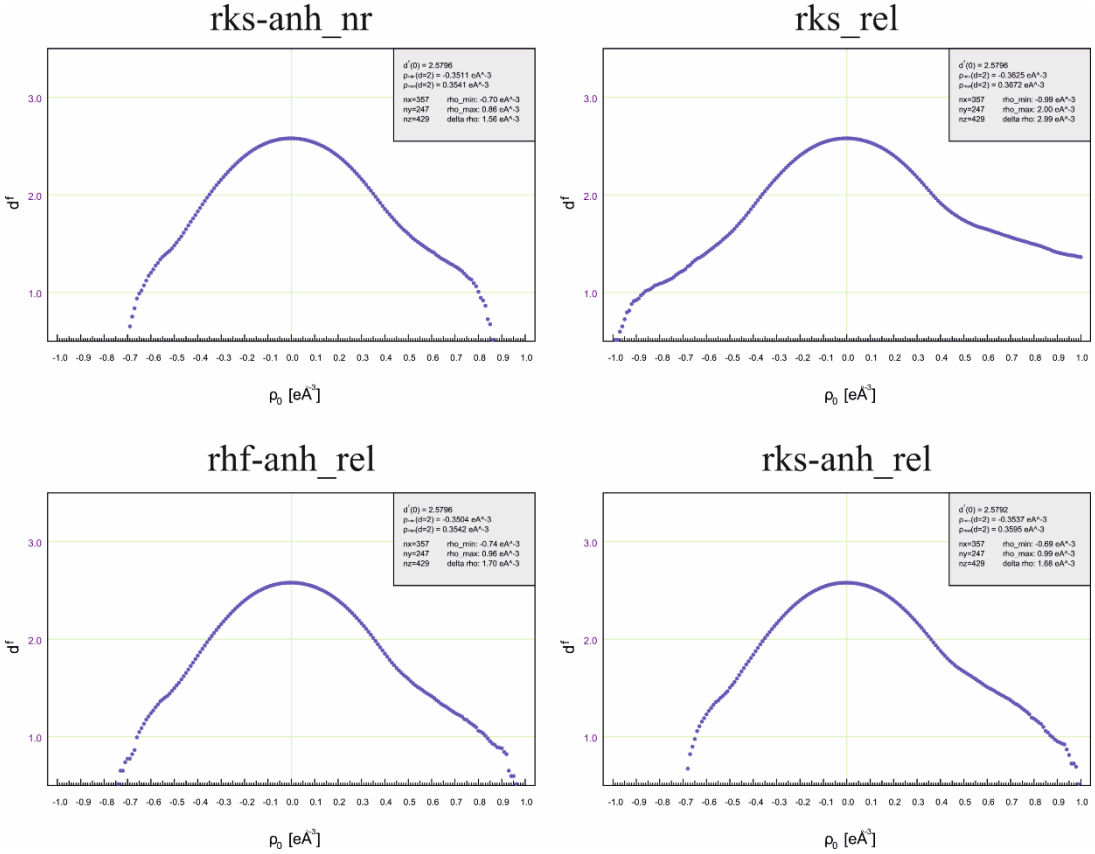


**Figure S12**The fractal dimension plots of the residual electron density resulting from HAR performed against SP8 data.

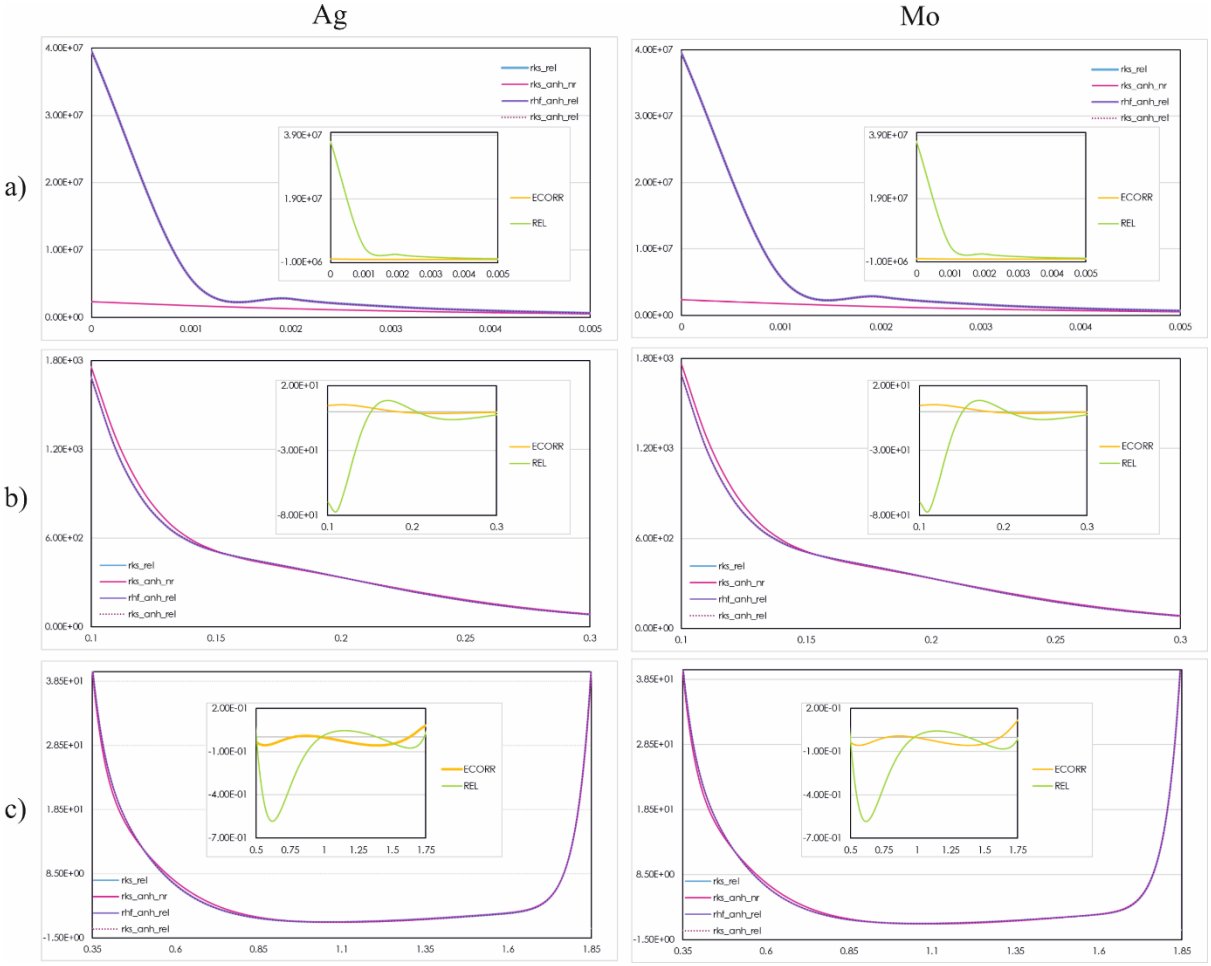


**Figure S13** 1D plots of electron density (y-axis, in eÅ-3) as a function of the Au−C bond distance (x-axis, in Å) resulting from HARs performed against Ag and Mo data. The subplots represents 1D difference plots resulting from the relativistic effects and electron correlation.

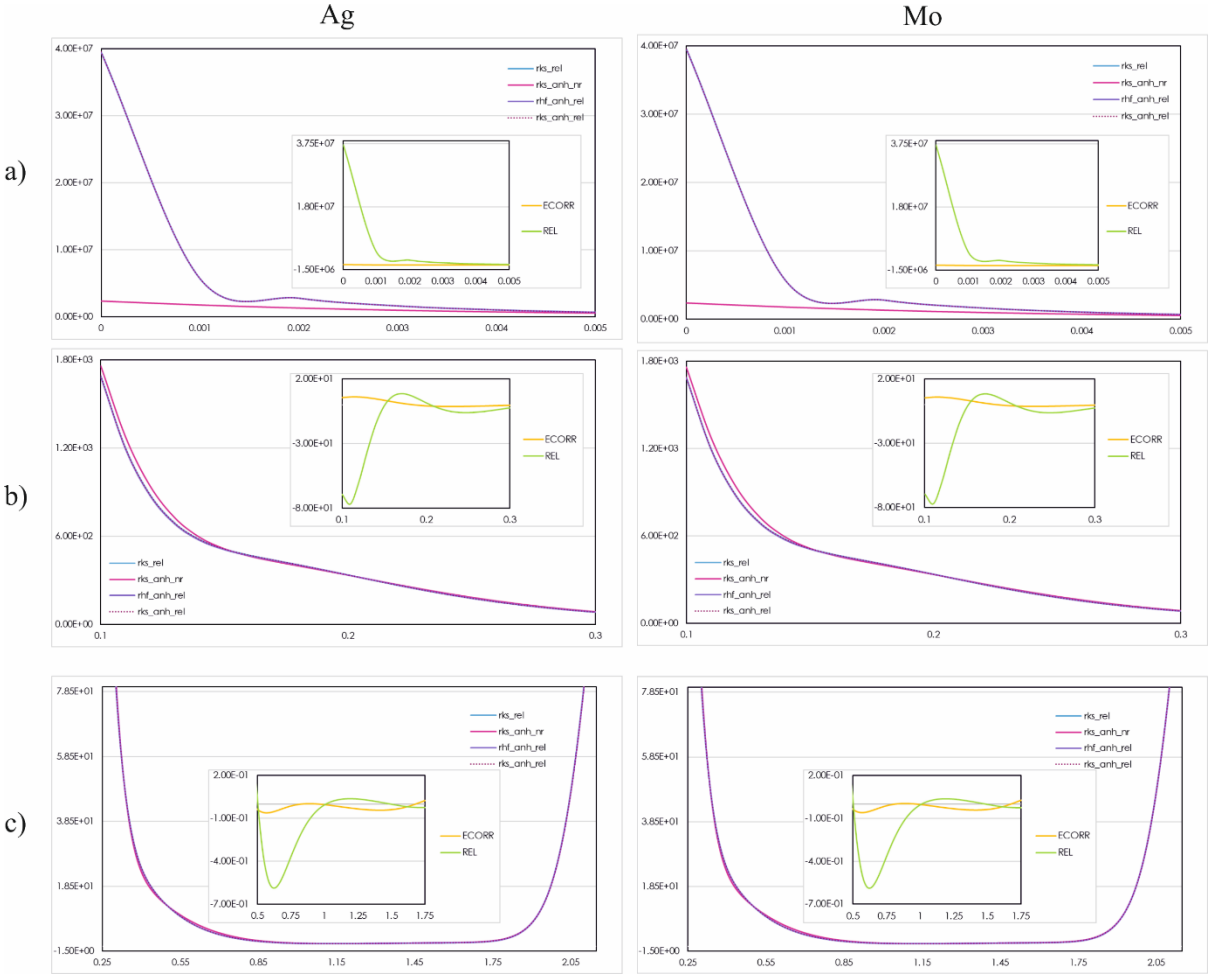


**Figure S14**1D plots of electron density (y-axis, in eÅ-3) as a function of the Au–P bond distance (x-axis, in Å) resulting from HARs performed against Ag and Mo data. The subplots represents 1D difference plots resulting from the relativistic effects and electron correlation.

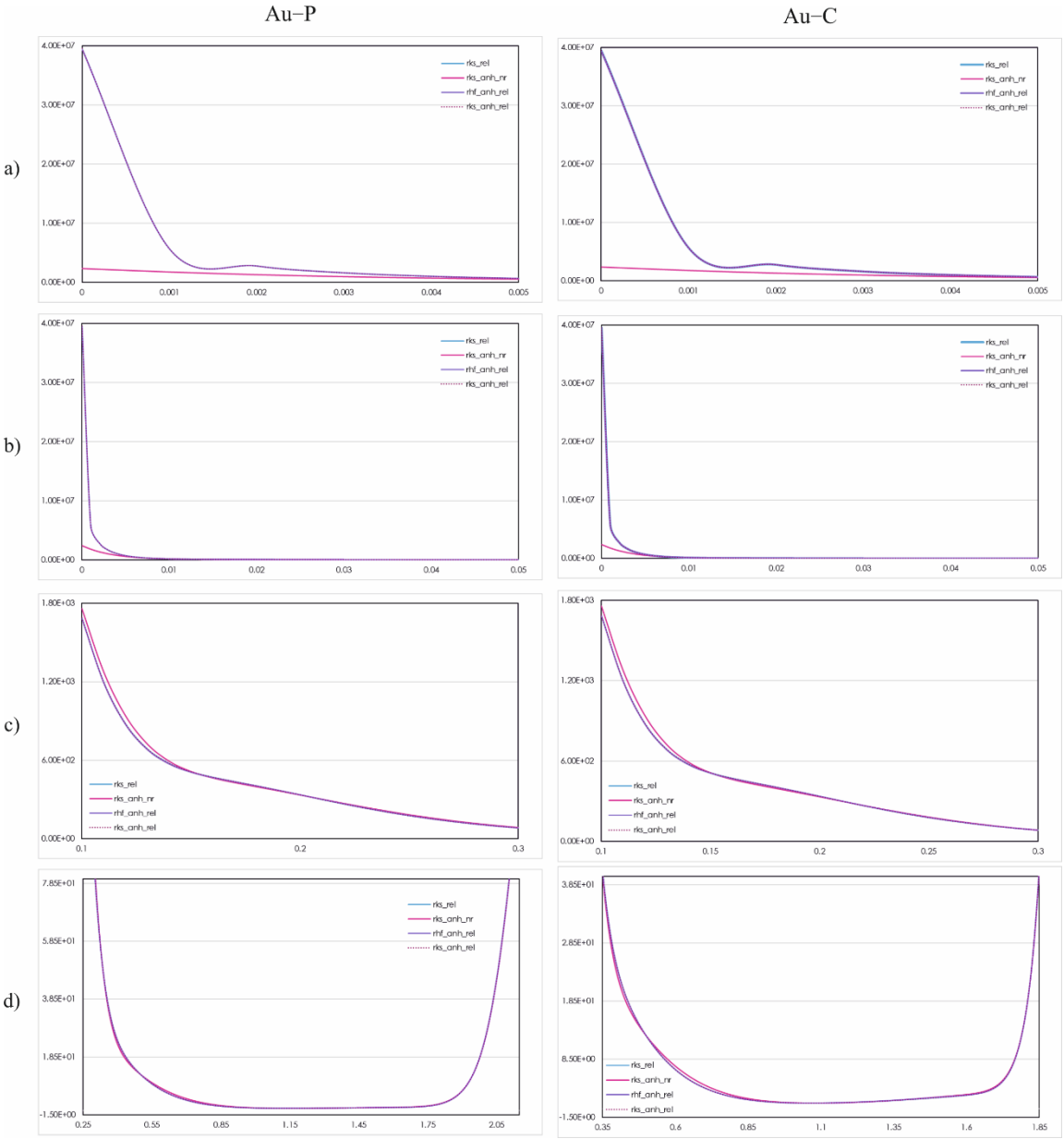


**Figure S15**1D plots of electron density (y-axis, in eÅ-3) as a function of the Au–P and Au–C bond distance (x-axis, in Å) resulting from HARs performed against SP8 data.

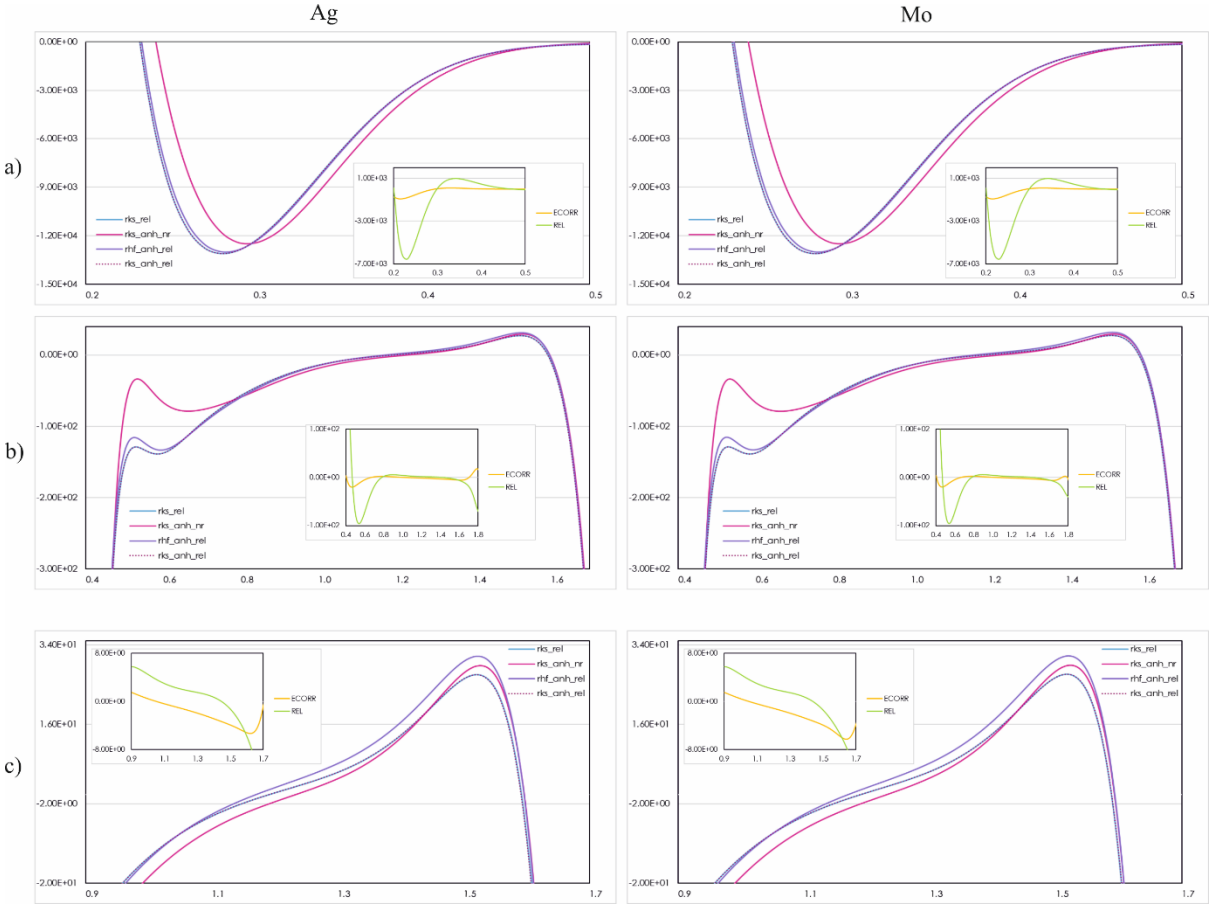


**Figure S16** 1D plots of negative Laplacian (y-axis, in eÅ$^{-5}$) as a function of the Au–C bond distance (x-axis, in Å) resulting from performed HARs against Ag and Mo data. The subplots show difference electron densities resulting from the relativistic and electron correlation effects.

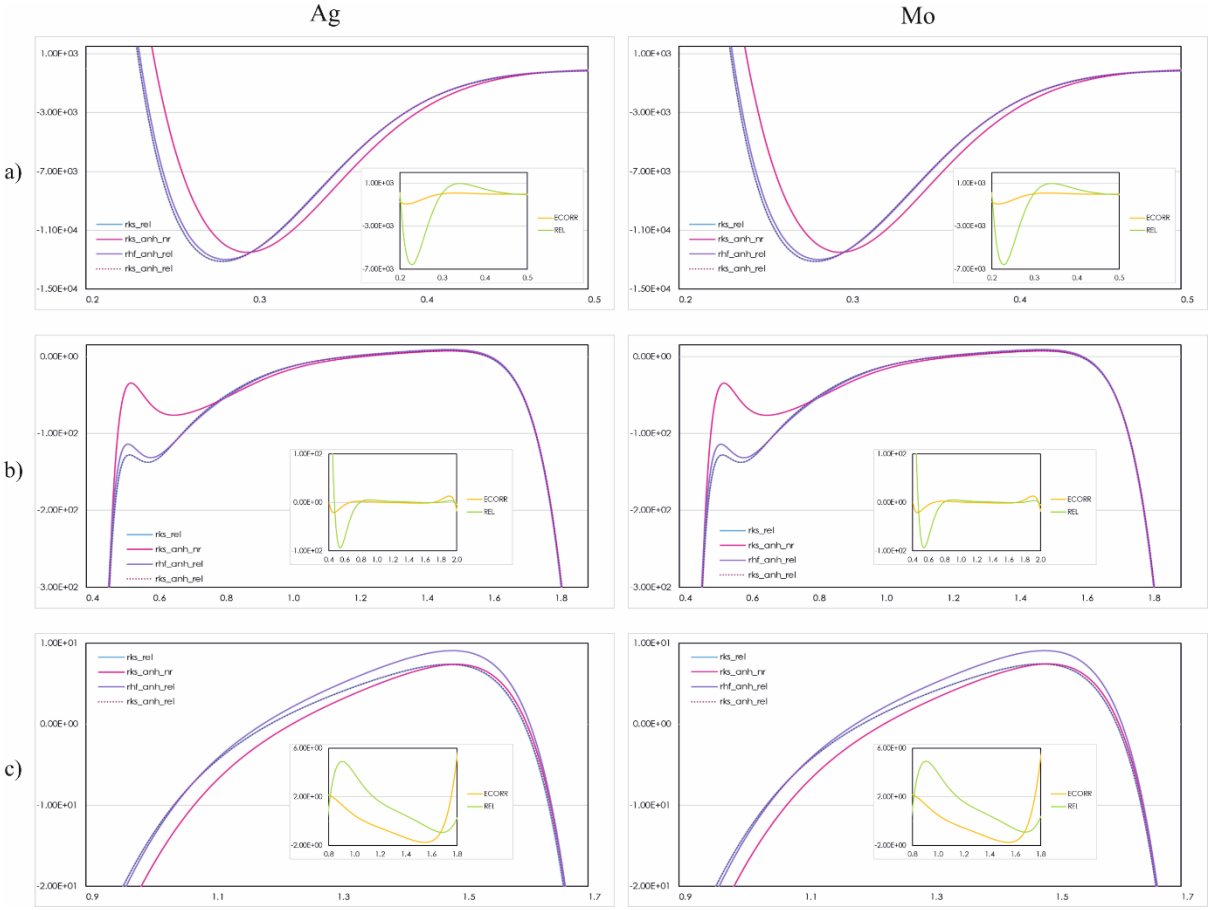


**Figure S17** 1D plots of negative Laplacian (y-axis, in eÅ$^{-5}$) as a function of the Au–P bond distance (x-axis, in Å) resulting from performed HARs against Ag and Mo data. The subplots show difference electron densities resulting from the relativistic and electron correlation effects.